ISSN 1070-3284, Russian Journal of Coordination Chemistry, 2013, Vol. 39, No. 1, pp. 82–86. © Pleiades Publishing, Ltd., 2013.

Solventothermal Syntheses, Structures and Photoluminescence of Two-Dimensional Lanthanide Coordination Polymers with Adipic Acid[1]

Q. Z. Huang[a], M. Li[b], Y. Q. Feng[a], and H. Z. Shi[a, *]

[a] *College of Chemistry and Pharmacy Engineering, Nanyang Normal University, Nanyang, 473061 P.R. China*

[b] *Department of Chemistry, Henan Institute of Education, Zhengzhou, 450046 P.R. China*

**e-mail: hzshi@nynu.edu.cn*

Received June 16, 2011

Abstract—Four lanthanide coordination polymers formulated as $[Ln_2(Ad)_3(H_2O)_4] \cdot 0.25H_2O$ (Ln = Tb (**I**), Pr (**II**), Ho (**III**), Dy (**IV**); H_2Ad = adipic acid), have been solventothermally synthesized from the self-assembly of the lanthanide ions (Ln^{3+}) with the exible adipic dicarboxylate ligand. All of them were characterized by IR spectroscopy and single-crystal X-ray diffraction. Structural analyses revealed that these complexes had intricate two-dimensional interpenetrated metal-organic networks. In addition, the photoluminescent properties of complex **I** was discussed in detail, which shows strong green emission, corresponds to $^5D_4 \rightarrow {}^7F_5$ transition of Tb^{3+} ions.

DOI: 10.1134/S1070328412100053

INTRODUCTION

In recent years, the design and construction of novel lanthanide organic frameworks have developed into an increasingly popular field, not only because of their intriguing topological structures but also due to their potential applications in a wide variety of fields such as luminescence [1], magnetism [2, 3], catalysis [4] and gas absorption and separation [5]. Lanthanide ions are good candidates to provide unique opportunities for the discovery of unusual network topologies due to their high affinity for hard donor atom, such as oxygen, nitrogen or hybrid oxygen-nitrogen atoms. On the basis of this inherent coordinating nature, many different kinds of exible aliphatic dicarboxylate ligands with long carbon-chain such as succinic acid, glutaric acid and adipic acid, etc, as building blocks, have a large variation in coordination behavior including chelating, bidentate-bridging or chelating-bridging modes, which allows for the formation of clusters, cage structures or open frameworks. Amongst these aliphatic dicarboxylate ligands, adipic acid ligand has a medium size carbon chain between terminal carboxylate groups, which has attracted increasing attention. However, in virtue of large radii, hydrolytic character in aqueous solution for lanthanide ions, the assembly of lanthanide-adipate coordination polymers may encounter many difficulties and great challenges. To the best of our knowledge, only a few lanthanide-adipate coordination polymers [6–9] have been synthesized mostly by a double diffusion silica gel technique and hydrothermal technique. In this paper, four new lanthanide-adipate coordination polymers, $[Ln_2(Ad)_3(H_2O)_4] \cdot 0.25H_2O$ (Ln = Tb (**I**), Pr (**II**), Ho (**III**), Dy (**IV**); H_2Ad = adipic acid) were solventothermally synthesized. Amongst these synthesis methods, the mixed solvents of ethanol/water with volume ratio of 1 : 2 was used for **II**, acetonitrile/water with volume ratio of 3 : 2 for **III** and **IV**, while for synthesis of **I**, water was utilized as solvent by two steps. In comparison with a double diffusion silica gel method, solventothermal synthesis with utilization of mixed solvents is a more effective and timesaving technique. The coexistence of water with organic solvent as a low dielectric media may effectively reduce solvent polarity so as to depress the lanthanide ions solvation, and resultantly increase ion transport ability and change the behavior of crystallizing thermodynamics and nucleation kinetics, which greatly benefits the construction of lanthanide-adipate coordination compounds.

EXPERIMENTAL

All chemicals were used as purchased without further purification. The FTIR spectra were obtained using a Nicolet 5700 FTIR spectrometer using KBr pellets.

Synthesis of I. $Tb(NO_3)_3 \cdot 6H_2O$ (0.2717 g, 0.6 mmol), H_2Ad (0.1314 g, 0.9 mmol) were dissolved in 15 mL H_2O. The resulting solution was added in a 50 mL Teflon-lined stainless steel vessel and heated under autogenous pressure at 160°C for 3 days and then cooled to room temperature. The resulting transparent solution was evaporated at room temperature for

[1] The article is published in the original.

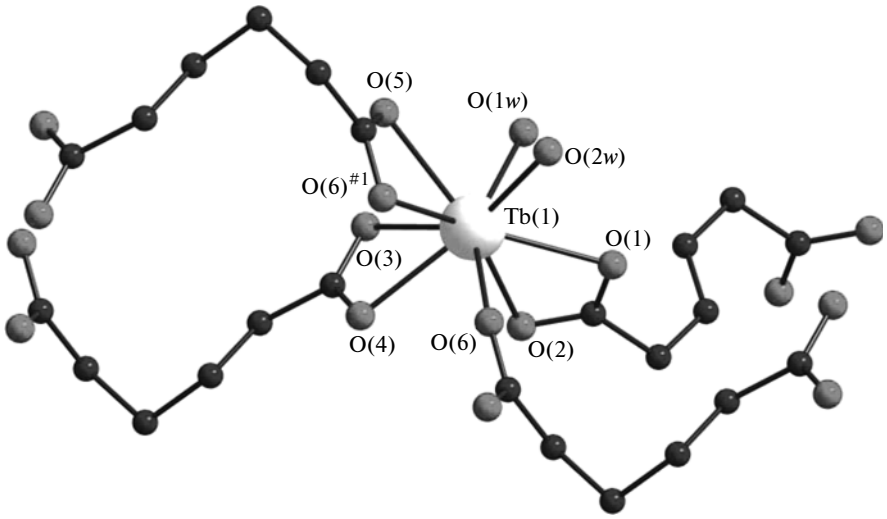

Fig. 1. Coordination environment of Tb in complex **I** with nonhydrogen atoms drawn by diamond (symmetry codes: #1 $0.5 - x$, $0.5 - y$, $-z$).

2 days. The colorless crystals were obtained. IR (KBr; ν, cm^{-1}): 3322, 2956, 1657, 1541, 1461, 1384, 646.

Synthesis of II. $Pr(NO_3)_3 \cdot 6H_2O$ (0.4349 g, 1 mmol), H_2Ad (0.2923 g, 2 mmol) were dissolved in 30 mL mixed solvent of ethanol/H_2O (2 : 1, v/v). The resulting solution was added in a 50 mL Teflon-lined stainless steel vessel and heated under autogenous pressure at 140°C for 3 days and then cooled to room temperature. The green crystals were obtained. IR (KBr; ν, cm^{-1}): 3331, 2954, 1659, 1538, 1441, 1314, 648.

Synthesis of III. $Ho(NO_3)_3 \cdot 6H_2O$ (0.2754 g, 0.6 mmol), H_2Ad (0.1314 g, 0.9 mmol) were dissolved in 25 mL mixed solvent of acetonitrile/H_2O (3 : 2, v/v). The resulting solution was added in a 50 mL Teflon-lined stainless steel vessel and heated under autogenous pressure at 110°C for 2 days and then cooled to room temperature. The colorless crystals were obtained. IR (KBr; ν, cm^{-1}): 3247, 2953, 1660, 1536, 1441, 1312, 649.

Synthesis of IV. $Dy(NO_3)_3 \cdot 6H_2O$ (0.2739 g, 0.6 mmol), H_2Ad (0.1314 g, 0.9 mmol) were dissolved in 25 mL mixed solvent of acetonitrile/H_2O (3 : 2, v/v). The resulting solution was added in a 50 mL Teflon-lined stainless steel vessel and heated under autogenous pressure at 110°C for 2 days and then cooled to room temperature. The pale violet crystals were obtained. IR (KBr; ν, cm^{-1}): 3325, 2952, 1654, 1542, 1458, 1387, 656.

X-ray single-crystal analyses. Suitable single crystals were carefully selected under a microscope. Crystal structure determinations for complexes **I**–**IV** were performed on a Bruker APEX-II CCD area detector with MoK_α monochromated radiation ($\lambda = 0.71073$ Å) at 296(2) K. The structure was solved by the direct method and refined by the full-matrix least-squares on F^2 using the SHELXTL-97 software. All of the nonhydrogen atoms were refined anisotropically. The organic hydrogen atoms were generated geometrically. The crystal data and structure refinement for complexes **I**–**IV** are provided in table.

Supplementary materials for complexes **I**–**IV** have been deposited with the Cambridge Crystallographic Data Centre (nos. 778984, 778982, 783557, 783555; deposit@ccdc.cam.ac.uk or http://www.ccdc.cam.ac.uk).

RESULTS AND DISCUSSION

Compound **I**–**IV** never be synthesized before. Therefore, compound **I** is taken as an example to present and discuss the structure in detail because they are isostructural. The Tb^{3+} coordination mode of **I** is shown in Fig. 1. Each Tb^{3+} cation has the same nine coordinate environment and is surrounded by nine oxygen atoms from three chelating bidentate carboxyl group (O(1), O(2), O(3), O(4), O(5), and O(6)), one dimonodentate carboxyl group $(O(6)^{\#1})$ from adipate ligands and two coordinated water molecules. The average Tb(1)–O bond distance of $TbO_7(H_2O)_2$ polyhedra gives 2.48 Å and the largest Tb–$O(6)^{\#1}$ of 2.65 Å results from edge-sharing Tb(1)–O bond. The distances of Tb(1)–O vary in the range of 2.395 to 2.653 Å. In the metal-organic networks, six $TbO_7(H_2O)_2$ polyhedra centers create 28-membered rings and 14-membered rings by connecting six adipate ligands (Fig. 2). In the 14-membered rings, two Tb^{3+} atoms are linked together via two adipate ligands with the Tb–Tb separation, bridged by adipic acid, is 9.173 Å. Furthermore, two other Tb^{3+} atoms are linked together via bridging carboxylate oxygen atoms form the two adipate ligands. The bridging mode of Tb^{3+} atoms

Crystal data and structure refinement for compounds **I**–**IV**

Parameter	Value			
	I	**II**	**III**	**IV**
Formula weight	826.71	790.69	838.73	833.87
Crystal system	Monoclinic	Monoclinic	Monoclinic	Monoclinic
Space group	*C*2/*c*	*C*2/*c*	*C*2/*c*	*C*2/*c*
a, Å	23.785(17)	23.820(10)	23.467(4)	23.524(12)
b, Å	14.233(10)	14.209(6)	13.960(2)	14.014(7)
c, Å	8.945(6)	8.873(4)	8.8031(15)	8.820(5)
β, deg	105.402(11)	105.361(6)	104.117(2)	104.220(8)
V, Å^3	2919(4)	2896(2)	2796.7(8)	2818(2)
Z	4	4	4	4
ρ_{calcd}	1.862	1.794	1.972	1.945
Size, mm	0.13 × 0.11 × 0.07	0.17 × 0.15 × 0.12	0.11 × 0.08 × 0.07	0.16 × 0.13 × 0.10
μ, cm^{-1}	4.871	3.391	5.685	5.329
F(000)	1568	1520	1584	1576
Scan mode	ω/2θ	ω/2θ	ω/2θ	ω/2θ
θ Range, deg	2.70–25.00	2.72 –25.00	1.79–25.00	2.75–24.99
Limiting indices *h*, *k*, *l*	$-28 \le h \le 28$, $-13 \le k \le 16$, $-10 \le l \le 10$	$-22 \le h \le 28$, $-15 \le k \le 16$, $-10 \le l \le 10$	$-27 \le h \le 27$, $-9 \le k \le 16$, $-10 \le l \le 10$	$-27 \le h \le 27$, $-16 \le k \le 14$, $-9 \le l \le 10$
Reflection collected	7245	7540	7000	7032
Independent reflections (R_{int})	2570 (R_{int} = 0.0400)	2551 (R_{int} = 0.0233)	2469 (R_{int} = 0.0275)	2482 (R_{int} = 0.0426)
Reflections with $I > 2\sigma(I)$	2193	2311	2139	2088
GOOF	1.039	1.159	1.123	1.060
R_1 ($I > 2\sigma(I)$)	0.0393	0.0302	0.0358	0.0421
R_1 (all data)	0.0471	0.0330	0.0417	0.0494
wR_2 ($I > 2\sigma(I)$)	0.1236	0.0980	0.1114	0.1354
wR_2 (all data)	0.1312	0.1008	0.1170	0.1431
$\Delta\rho_{min}/\Delta\rho_{max}$, *e* Å^{-3}	−1.668/2.508	−1.125/1.580	−2.172/ 2.685	−1.318/2.243

with oxygen from adipic acids are all type *b*. For the 28-membered ring, four Tb^{3+} atoms are linked together via four adipate ligands. The adjacent Tb^{3+} centers have a general separation of 8.945 and 10.309 Å, and the separation of cornerwise Tb^{3+} centers is 10.7721 and 16.0169 Å. Furthermore, the bridging modes of adipic acids with Tb^{3+} consist of two types and the ratio of type *a* to *b* is 1 : 1 (Fig. 3). The 28-membered ring and 14-membered ring linked together, which forms a repetitive constituent. The most interesting feature is that these repetitive constituents can interweave together along two different directions (Fig. 4), which generates the so-called inclined interpenetration mode equivalent to a (4,4) topologically network with the dihedral angle of 50.929°C between the interpenetrating layers and produced an interlocked two-dimensional structure (Fig. 5).

Lanthanide coordination polymers are interesting luminescence materials because their emissions cover the entire spectrum: near-infrared (Nd^{3+}, Er^{3+}), red

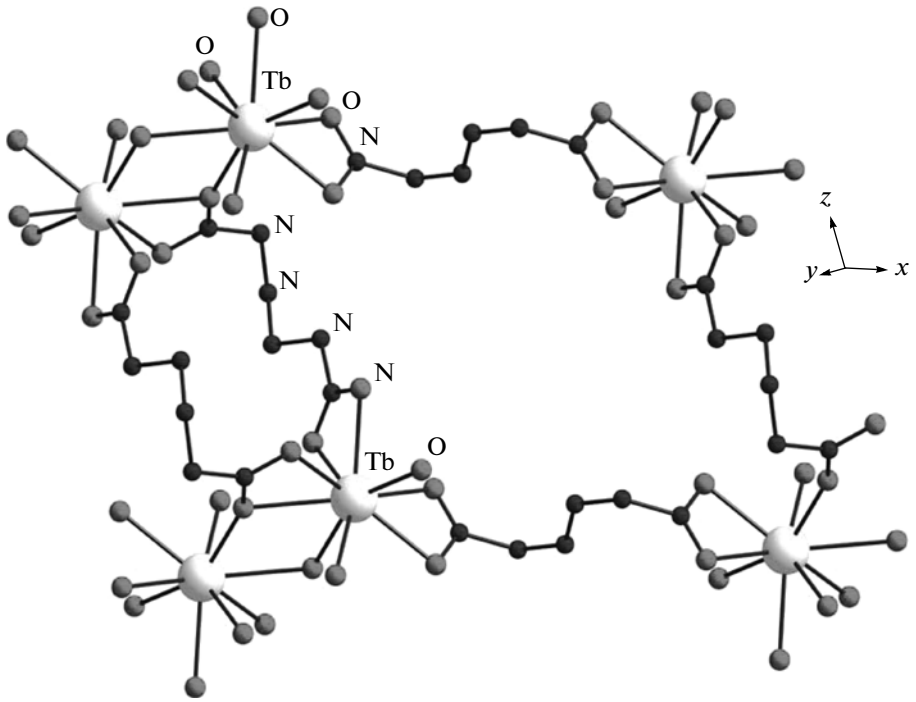

Fig. 2. View of the repetitive constituent formed with 36-membered ring and 18-membered ring linked together in **I**.

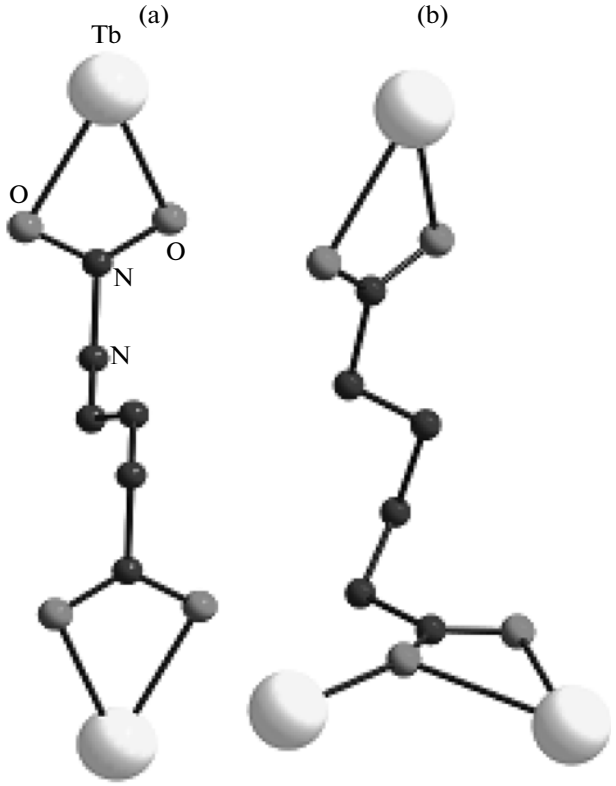

Fig. 3. Two distinct ligand conformations (a) and (b) observed in complex **I**.

(Eu^{3+}, Pr^{3+}, Sm^{3+}), green (Er^{3+}, Tb^{3+}) and blue (Tm^{3+}, Ce^{3+}) [10–16], in which the energy transfer from the organic ligands to Eu^{3+} and Tb^{3+} is more effective.

The solid-state luminescent property of complex **I** was carried out at room temperature. When excited at 349 nm for **I**, it emits green light luminescence (Fig. 6).

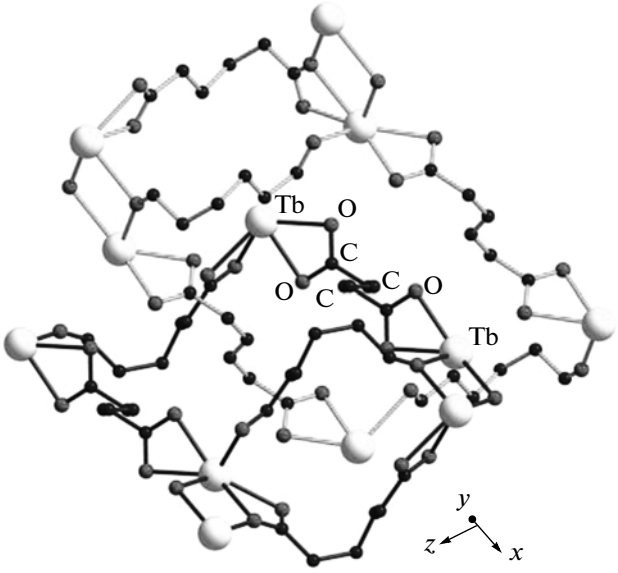

Fig. 4. View of the interpenetration of two repetitive constituents in **I**.

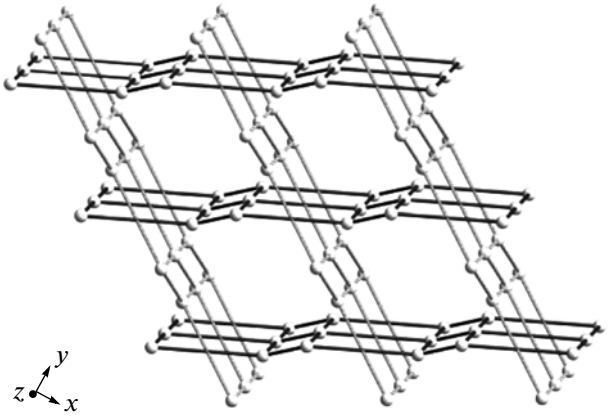

Fig. 5. The diagram of the 2D supramolecular interpenetrating network in **I**.

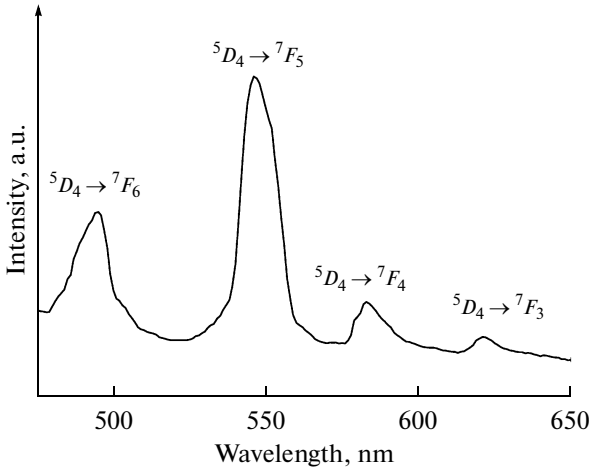

Fig. 6. Room-temperature solid-state photoluminescence spectra of complex **I**.

The emission spectrum of complex **I** reveals four main peaks located at 489, 543, 587 and 618 nm, corresponding to the $^5D_4 \rightarrow {}^7F_6$, $^5D_4 \rightarrow {}^7F_5$, $^5D_4 \rightarrow {}^7F_4$ and $^5D_4 \rightarrow {}^7F_3$ transition emission of the Tb^{3+} ion, respectively. The strongest emission is centered on 543 nm ($^5D_4 \rightarrow {}^7F_5$), which is responsible for the green emission.

ACKNOWLEDGMENT

This study is nancially supported by scientific and technological department of Henan Province (no. 102300410269).

REFERENCES

1. Lill, D.T., Bettencourt-Dias, A., and Cahill, C.L., *Inorg. Chem.*, 2007, vol. 46, p. 3960.
2. Li, Z.Y., Zhu, G.S., Guo, X.D., et al., *Inorg. Chem.*, 2007, vol. 46, p. 5174.
3. Cheng, J.W., Zhang, J., Zheng, S.T., and Yang, G.Y., *Chem. Eur. J.*, 2008, vol. 14, p. 88.
4. Gandara, F., Andres, A., Gomez-Lor, B., et al., *Cryst. Growth Des.*, 2008, vol. 8, p. 378.
5. Chen, X.Y., Zhao, B., Shi, W., et al., *Chem. Mater.*, 2005, vol. 17, p. 2866.
6. Duan, L.M., Xu, J.Q., Xie, F.T., et al., *Inorg. Chem. Commun.*, 2004, vol. 7, p. 216.
7. Michaelides, A. and Skoulika, S., *Cryst. Growth Des.*, 2009, vol. 9, p. 2039.
8. de Lill, D.T., de Bettencourt-Dias, A., and Cahill, C.L., *Inorg. Chem.,* 2007.
9. Wang, C.G., Xing, Y.H., Li, Z.P., et al., *Cryst. Growth Des.*, 2009, vol. 9, p. 1525.
10. Wang, X.J., Cen, Z.M., Ni, Q.L., et al., *Cryst. Growth Des.*, 2010, vol. 10, p. 2960.
11. Xie, Y., Xing, Y.H., Wang, Z., et al., *Inorg. Chim. Acta*, 2010, vol. 363, p. 918.
12. Wang, Z., Bai, F.Y., Xing, Y.H., et al., *Inorg. Chim. Acta*, 2010, vol. 363, p. 669.
13. Xia, J., Zhao, B., Wang, H.S., et al., *Inorg. Chem.*, 2007, vol. 46, p. 3450.
14. Zhang, X.J., Xing, Y.H., Han, J., et al., *Cryst. Growth Des.*, 2008, vol. 8, p. 3680.
15. Wang, H.S., Zhao, B., Zhai, B., et al., *Cryst. Growth Des.*, 2007, vol. 7, p. 1851.
16. Wang, H.S., Zhao, B., Zhai, B., et al., *Cryst. Growth Des.*, 2007, vol. 7, p. 1851.